Electronic Supplementary Information (ESI) for Nanoscale.
This journal is © The Royal Society of Chemistry 2017

Supporting Information for

Novel Fe-N-C catalyst for efficient oxygen reduction reaction based on polydopamine nanotubes

Feng Tang, Haitao Lei, Shujun Wang, Huixin Wang and Zhaoxia Jin*

Department of Chemistry, Renmin University of China, Beijing, 100872 (P. R. China)

E-mail of corresponding author: jinzx@ruc.edu.cn

Supporting Materials Contain Following Sections:

1. Figures

Fig. S1. XRD patterns of FNCT catalysts. p3

Fig. S2. SEM and TEM image of NCT800. .....p3

Fig. S3. Raman spectra of FNCT catalysts. p3

Fig. S4-S5. N_2 absorption-desorption curves of FNCT catalysts. p4

Fig. S6. TGA curves of FNCT catalysts. p4

Fig. S7. XRD patterns of TGA residue of FNCT800-100. .....p5

Fig. S8. XPS spectrum of NCT800. .....p5

Fig. S9. LSV curves of commercial Pt/C and NCT800. .....p5

Fig. S10-S15. LSV curves of FNCT catalysts and corresponding electron transfer numbers. p6

Fig. S16. Characterization results of ball milling-acid leaching experiment. p8

Fig. S17. LSV curves for the determination of collection efficiency N of RRDE. p8

2. Tables

Table S1. Loading amount of Fe in different FNCT catalysts calculated based on TGA. p9

Table S2. Comparison of ORR performance for different non-precious N-doped PCMs catalysts reported in recent literatures. p9

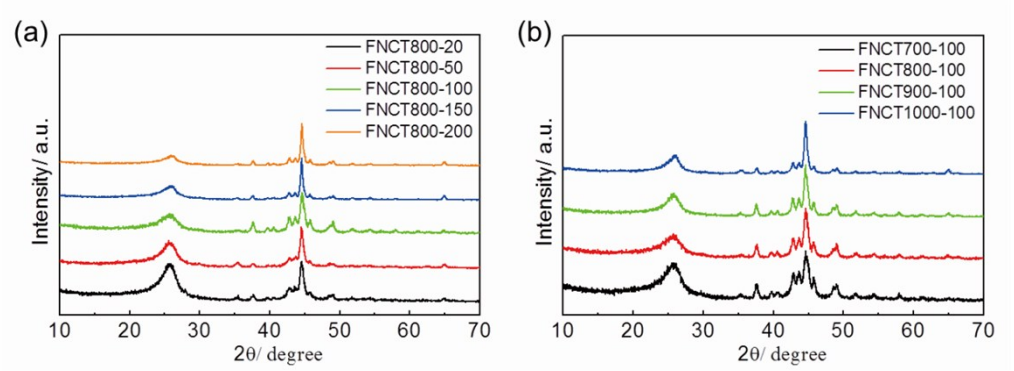

Fig. S1 XRD patterns of different catalysts prepared at different experimental conditions. (a) Various amount of iron source and (b) Different pyrolysis temperatures.

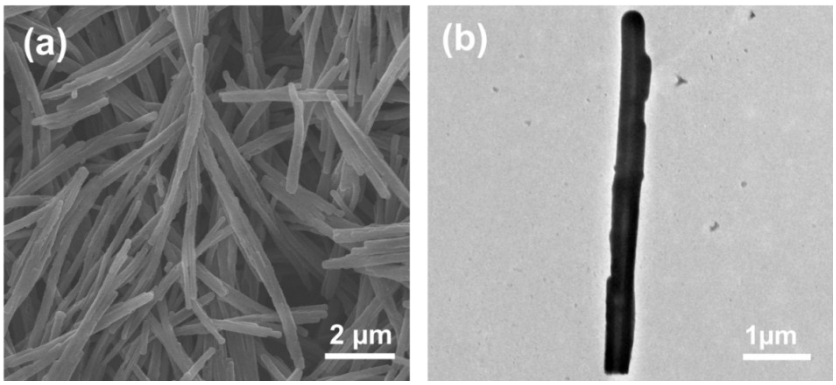

Fig. S2 (a) SEM image and (b) TEM image of NCT800.

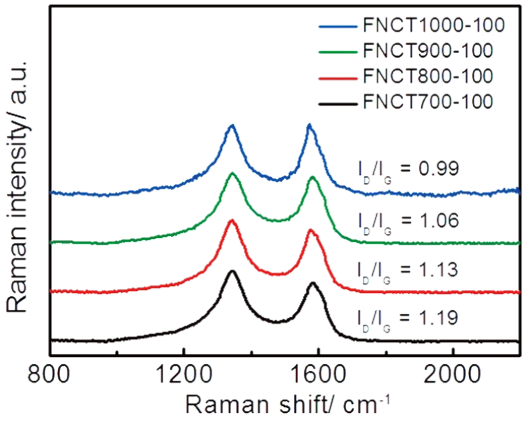

Fig. S3 Raman spectra of different catalysts prepared at various pyrolysis temperatures.

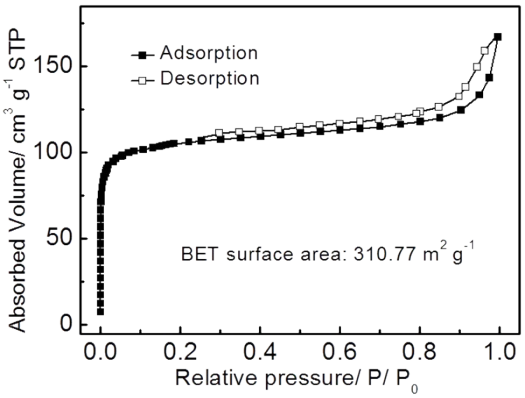

Fig. S4 N_2 absorption-desorption curves of NCT800.

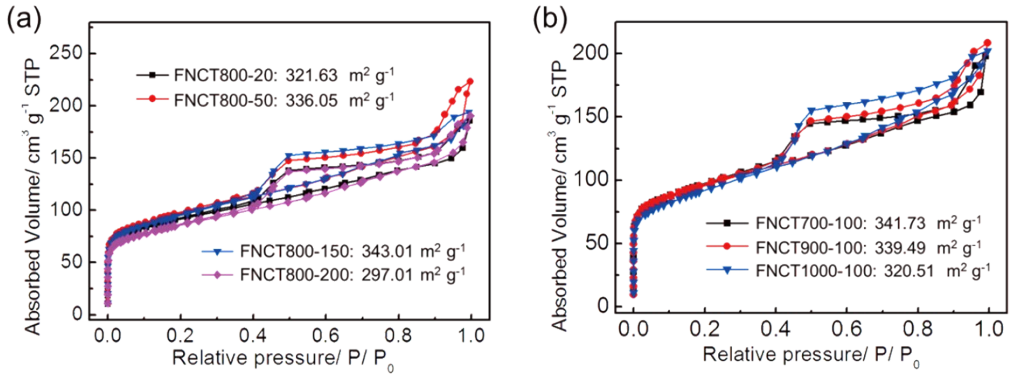

Fig. S5 N_2 absorption-desorption curves of different FNCT catalysts prepared at different experimental conditions. (a) Different amount of iron source and (b) Various pyrolysis temperatures.

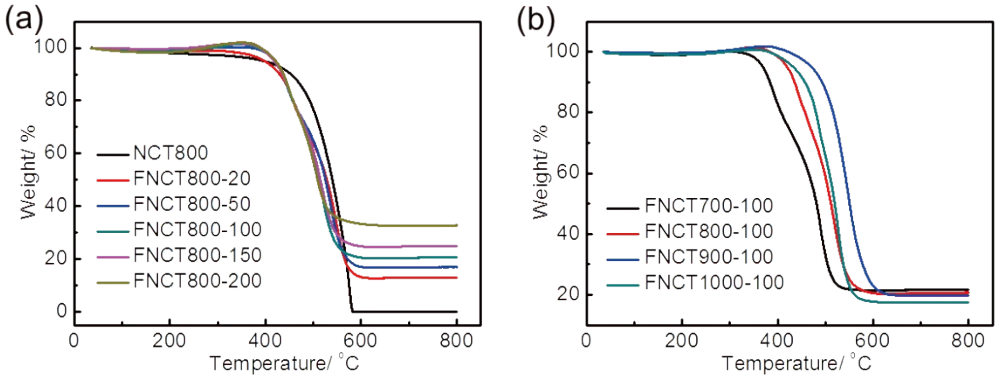

Fig. S6 TGA curves of different FNCT catalysts prepared at different experimental conditions. (a) Various amount of iron source and (b) Different pyrolysis temperatures.

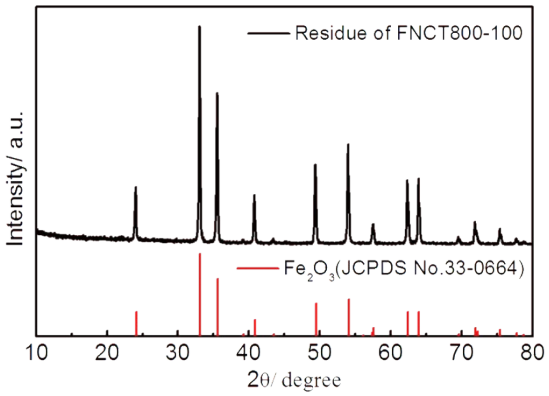

Fig. S7 XRD pattern of TGA residue of FNCT800-100.

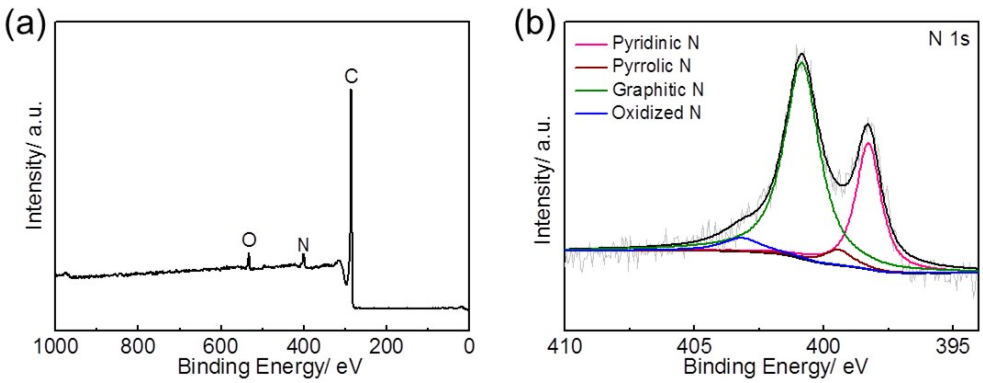

Fig. S8 XPS survey of NCT800 and corresponding high-resolution XPS spectra of N 1s.

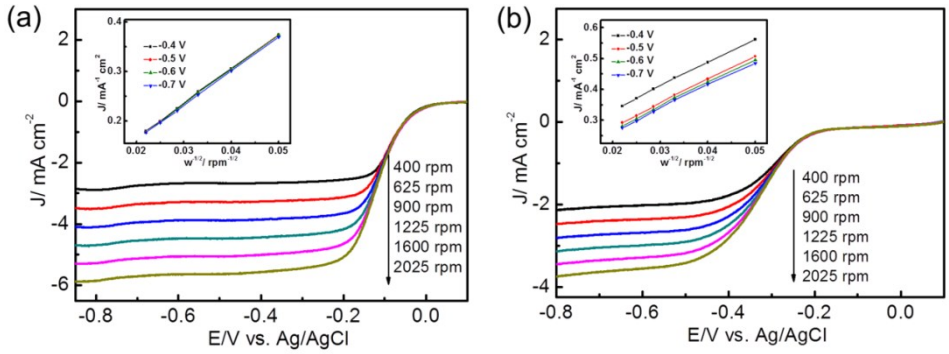

Fig. S9 LSV curves of (a) commercial Pt/C and (b) NCT800 with various rotation rates. The insets show the corresponding K-L plots at different electrode potentials.

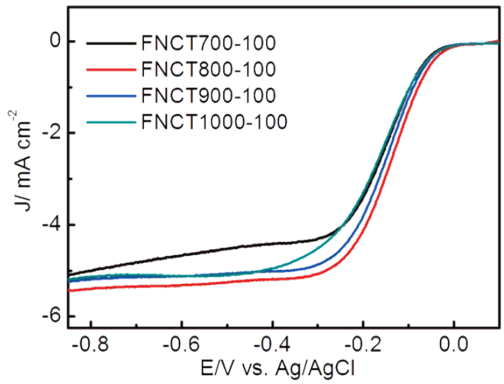

Fig. S10 LSV curves of FNCT catalysts prepared at various pyrolysis temperatures in O_2-saturated 0.1 M KOH aqueous solution at a scan rate of 1600 rpm.

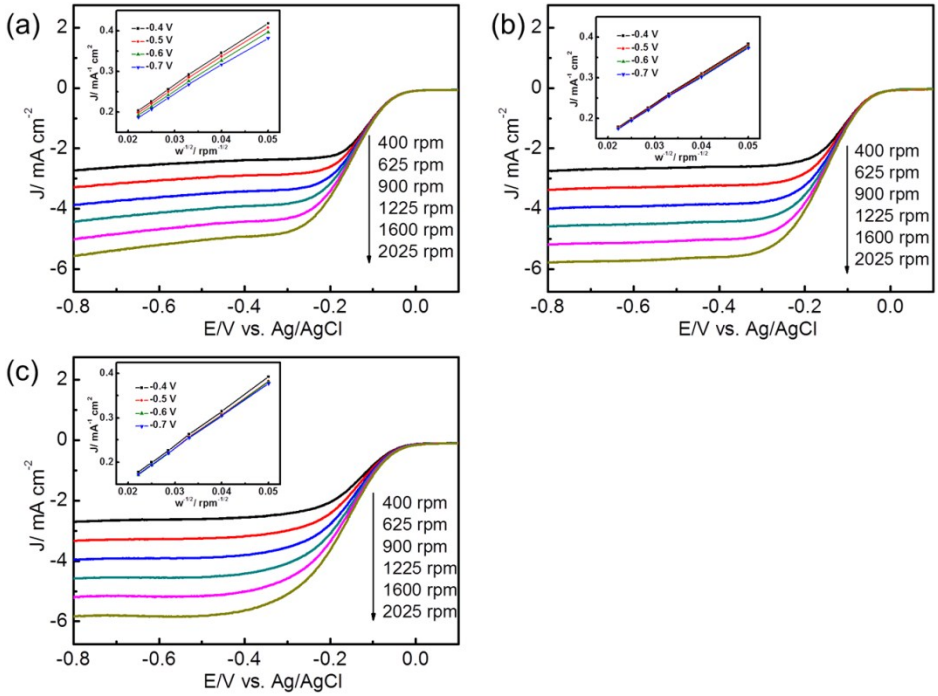

Fig. S11 LSV curves of (a) FNCT700-100, (b) FNCT900-100 and (c) FNCT1000-100 with various rotation rates. The insets show the corresponding K-L plots at different electrode potentials.

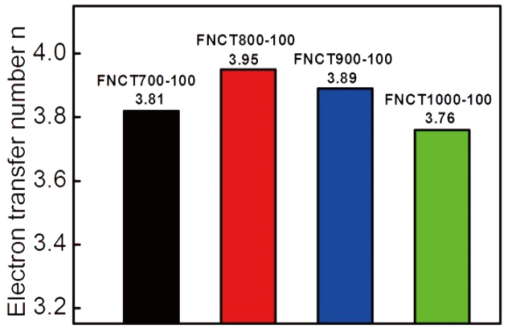

Fig. S12 Electron transfer numbers of different catalysts prepared at various pyrolysis temperatures derived from their corresponding LSV curves at a scan rate of 1600 rpm.

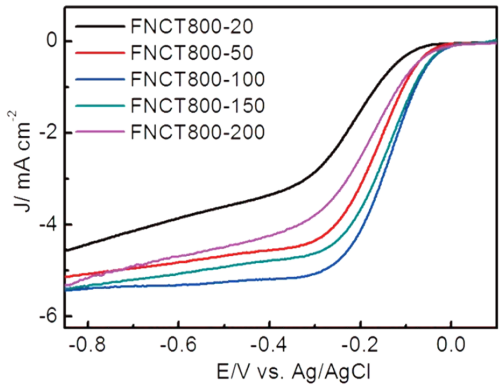

Fig. S13 LSV curves of FNCT catalysts prepared at 800 °C with various amount of iron source in O_2-saturated 0.1 M KOH aqueous solution at a scan rate of 1600 rpm.

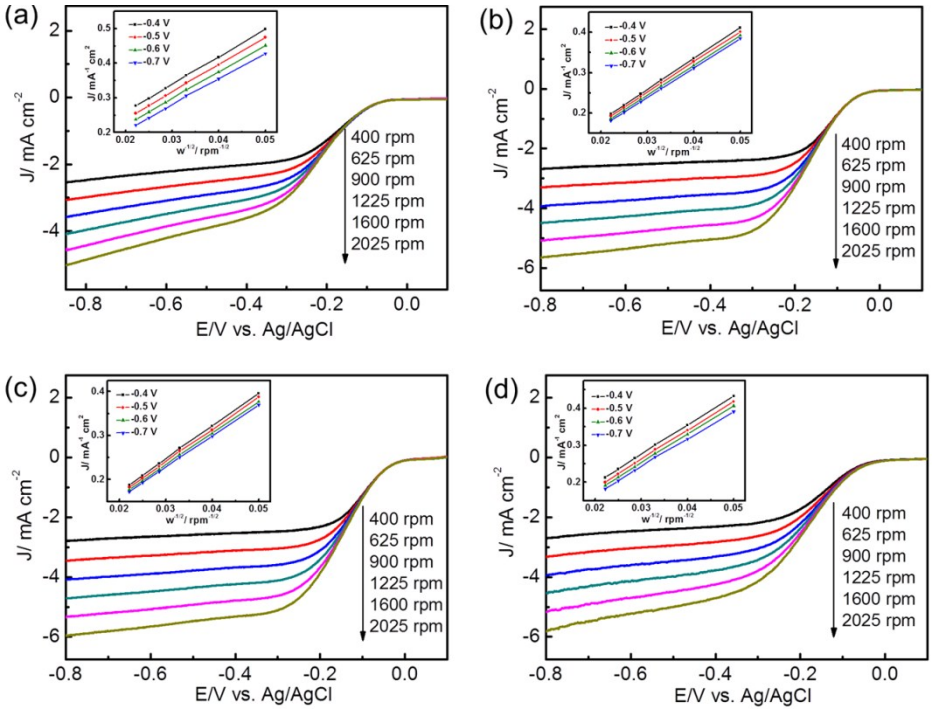

Fig. S14 LSV curves of (a) FNCT800-20, (b) FNCT800-50, (c) FNCT800-150 and (d) FNCT800-200 with various rotation rates. The insets show the corresponding K-L plots at different electrode potentials.

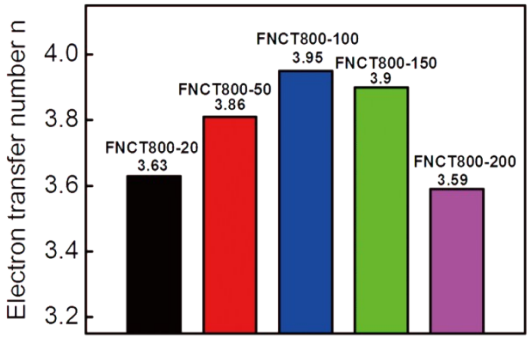

Fig. S15 Electron transfer numbers of different catalysts prepared at 800 °C with various amount of iron source derived from their corresponding LSV curves at a scan rate of 1600 rpm.

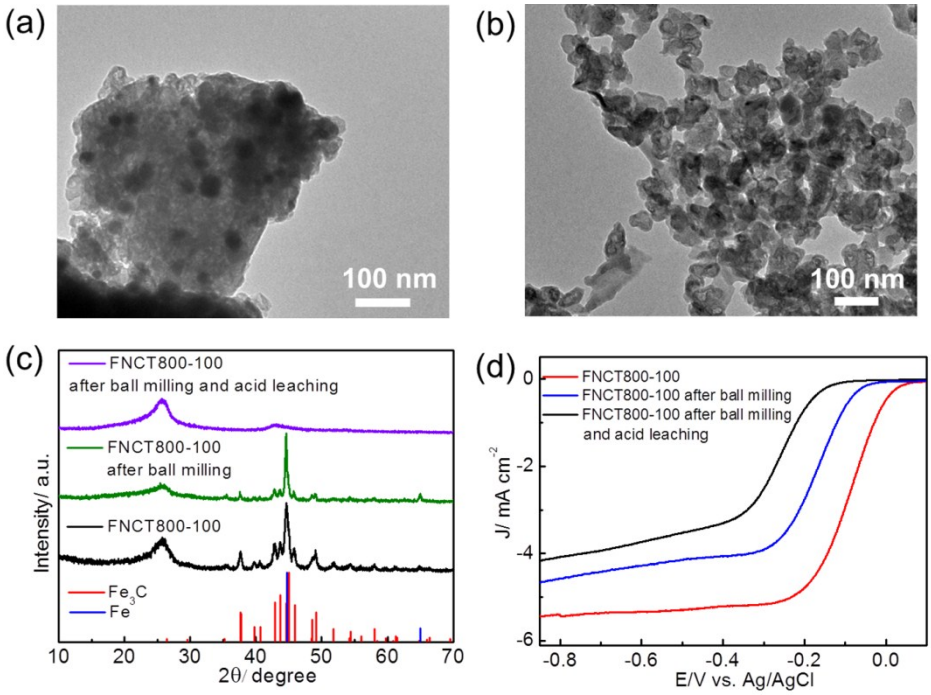

Fig. S16 TEM image of FNCT800-100 after ball milling (a) and following acid leaching (b). XRD patterns (c) and polarization curves of FNCT800-100, ball-milled FNCT800-100, and ball-milled FNCT800-100 after acid leaching (d).

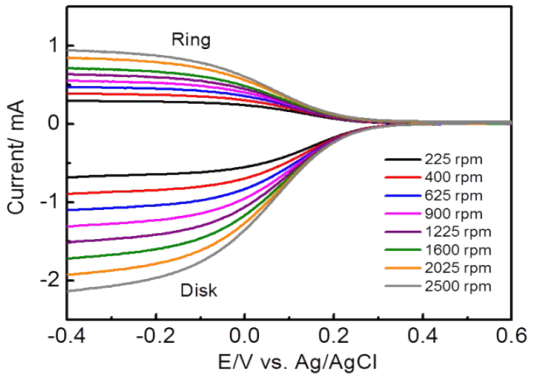

Fig. S17 LSV curves for the determination of collection efficiency *N* of RRDE. The N measurement was carried out in 0.1 M KOH with 2 mM $K_3Fe(CN)_6$ and 1 M KNO_3 as electrolyte and using a potential scanning rate of 10 mV s^{-1}. The calculated value 43.5% is close to the manufacture's value of 43%.

Table S1 Loading amount of Fe in different FNCT catalysts calculated from TGA.

Sample	Fe_2O_3 wt%	Corresponding Fe wt%
FNCT800-20	12.94	9.05
FNCT800-50	17.01	11.90
FNCT800-100	20.72	14.49
FNCT800-150	24.99	17.48
FNCT800-200	32.82	22.95
FNCT700-100	21.66	15.15
FNCT900-100	19.83	13.87
FNCT1000-100	17.43	12.19

Table S2 Comparison of ORR performance (V vs. Ag/AgCl) for different non-precious N-doped PCM catalysts reported in recent literatures.[a]

Catalysts	**E**		**Current Density**	**n**		**Ref.**
	E_{onset}	**$E_{1/2}$**	**at -0.6 V (mA cm^{-2})**	**K-L plot**	**RRDE**	
FNCT	-0.038 (0.933 vs. RHE)	-0.143 (0.828 vs. RHE)	-5.319	3.96	3.84-3.94	This work
NCF-Co	-0.09	-0.18	<-4.5	3.96	/	S1
Fe-N-CNP-CNF	-0.1	-0.19	/	3.9-4.1	3.61-3.88	S2
NDC	0.862 (vs. RHE)	/	<-4.3	4	/	S3
Fe-N-CNFs	-0.02	-0.14	-5.12 (at -0.7 V)	3.93-3.95	/	S4
Fe_3C@NCTs	0.098	-0.147	-3.1	3.8	/	S5
Co-N-C HHMT	0.973 (vs. RHE)	0.871 (vs. RHE)	-5.76	3.95-4.0	3.74-3.88	S6
NiCo@NCNT	0.93 (vs. RHE)	0.82 (vs. RHE)	/	3.7-3.9	/	S7
CNT@NPC	-0.114	-0.253	-5	>3.9	/	S8
N-CACNT-NF	-0.06	-0.168	/	3.98	/	S9
Co/N-CNT	0.94	0.84	/	3.85	/	S10
Fe/N-CNT	0.96 (vs. RHE)	0.82 (vs. RHE)	/	3.90	/	
Fe/N/C-HNSs	/	-0.22	/	3.8	/	S11
Fe_2N/MNGCS	0.960 (vs. RHE)	0.881 (vs. RHE)	/	4	/	S12
Z67D-700-L	/	<0.8 (vs. RHE)	/	3.5	/	S13

a. The potential, measured with Ag/AgCl (3.5 M KCl) reference electrode, was converted to the potential versus the reversible hydrogen electrode (RHE) according to the Nerst Equation:

$$E_{RHE} = E_{Ag/AgCl} + 0.0591\ pH + 0.203$$

[S1] J. Yan, H. Lu, Y. Huang, J. Fu, S. Mo, C. Wei, Y.-E. Miao and T. liu, *J. Mater. Chem. A*, **2015**, *3*, 23299.
[S2] G. Panomsuwan, N. Saito and T. Ishizaki, *RSC adv.* **2016**, *6*, 114553.
[S3] D. K. Singh, R. N. Jenjeti, S. Sampath and M. Eswaramoorthy, *J. Mater. Chem. A*, **2017**, *5*, 6025.
[S4] Z.-Y. Wu, X.-X. Xu, B.-C. Hu, H.-W. Liang, Y. Lin, L.-F. Chen and S.-H. Yu, *Angew. Chem. Int. Ed.*, **2015**, *54*, 8179.
[S5] G. Zhong, H. Wang, H. Yu and F. Peng, *J. Power Sources* **2015**, *286*, 496.
[S6] S. H. Ahn and A. Manthiram, *Small*, **2017**, 1603437.
[S7] L. Zeng, X. Cui, L. Chen, T. Ye, W. Huang, R. Ma, X. Zhang and J. Shi, *Carbon* **2017**, *114*, 347.
[S8] W.-J. Jiang, J.-S. Hu, X. Zhang, Y. Jiang, B.-B. Yu, Z.-D. Wei and L.-J. Wan, *J. Mater. Chem. A*, **2014**, *2*, 10154.
[S9] W. Zhao, P. Yuan, L. She, Z. Xia, S. Komarneni, K. Xi, Y. Che, X. Yao and D. Yang, *J. Mater. Chem. A*, **2015**, *3*, 14188.
[S10] Y. Liu, H. Jiang, Y. Zhu, X. Yang and C. Li, *J. Mater. Chem. A*, **2016**, *4*, 1694.
[S11] D. Zhou, L. Yang, L. Yu, J. Kong, X. Yao, W. Liu, Z. Xu and X. Lu, *Nanoscale*, **2015**, *7*, 1501.
[S12] X. Xiao, Y. Xu, Y. Xia, J. Xi and S. Wang, *Nano Energy*, **2016**, 2*4*, 121.
[S13] Y. Liu, H. Jiang, Y. Zhu, X. Yang and C. Li, *J. Mater. Chem. A*, **2016**, *4*, 1694.